Energy and Buildings 136 (2017) 173–188

Contents lists available at ScienceDirect

Energy and Buildings

journal homepage: www.elsevier.com/locate/enbuild

Experimental and analytical investigation of hydronic system retrofits in an urban high-rise mixed use building

Michael Waite*, Ankita Deshmukh, Vijay Modi

Department of Mechanical Engineering, Columbia University, USA

ARTICLE INFO

Article history:
Received 7 August 2016
Received in revised form 19 October 2016
Accepted 3 December 2016
Available online 7 December 2016

Keywords:
Building energy
Hydronic systems
Energy monitoring
Statistical engineering analysis
Constant and variable speed pumping
Flow control valves

ABSTRACT

As the size of buildings and demands on large centralized heating and cooling systems increases concurrent with rapid worldwide urbanization, the energy impact of hydronic distribution systems will become increasingly important in reducing greenhouse gas emissions. Further, in the U.S., the growth in multi-family buildings and the share of residential units in large multifamily buildings is far outpacing single-family construction. This paper describes a study of the pumping energy requirements of an urban 23-story mixed-use, primarily multifamily residential building before and after a suite of energy conservation measures. The retrofit focused on waterside technologies: Variable frequency drives (VFDs), constant and variable speed pumps, and pressure-independent control valves. In the original building, the central pumping equipment was found to be responsible for 55% of total annual owner-metered electricity usage and 29% of all annual owner-paid utility bills. Using extensive in-situ monitoring and analytical models developed for this effort, the full retrofit was computed to achieve a 41% reduction in annual central pumping electricity, representing an annual savings of 12% of all owner-paid energy bills. The most significant energy impact is attributable to the VFDs, and it can be inferred that additional savings could be achieved by installing VFDs on constant speed pumps.

1. Introduction

Buildings account for 41% of total U.S. primary energy usage [1]. Space conditioning (heating and cooling) and domestic hot water (DHW) represent more than 46% of primary energy usage (sometimes referred to as "source" energy) attributable to buildings. Multifamily residential buildings are fast becoming a critical component of this landscape: A 20 billion square feet increase in total U.S. multifamily residential floor area has been projected by 2021 relative to the 2011 building stock, compared to a 4 billion square feet *decrease* in total U.S. single-family residential floor area [2]. The potential complexity of multifamily building mechanical systems is of particular interest as the size of individual buildings increases: In 2014, 48% of all new multifamily residential units in the United States were in buildings that contain at least 50 residential units; 20 years earlier, the equivalent value was 8% [3].

With steam-based space heating systems difficult to deploy in complex structures [4] and not ideal for the heterogeneous loads of mixed building uses, the adoption of more flexible and controllable hot water distribution systems (i.e. hydronic systems) requires pumps to circulate the water [5]. Chilled water can also be similarly distributed to thermal zones from central mechanical refrigeration plants in large buildings [6].

With rapid worldwide urbanization [7], and the attractiveness and potential benefits of higher density living [8], new construction in cities is increasingly tall multifamily and mixed use buildings. According to data available from New York City [9], 49% of total citywide building floor area is in multifamily residential and mixed use buildings; 18% of total citywide building floor area is in high-rise[1] multifamily and mixed use buildings. In Manhattan, a high-density area and possible harbinger of future urban development, 37% of all building floor area is in high-rise multifamily and mixed use buildings.

The energy required to operate pumps across the building stock and for individual building types is difficult to estimate; one study commissioned by the U.S. Department of Energy estimated that 3%

* Corresponding author. Postal address: Mechanical Engineering Department, Columbia University, 220 S. W. Mudd Building, 500 West 120th Street, New York, NY 10027 USA.
E-mail address: mbw2113@columbia.edu (M. Waite).

[1] Throughout this paper, seven stories is used as the threshold for a high-rise building based on the NFPA Life Safety Code definition as a "building with an occupied floor located more than 75 feet above the lowest level of fire department vehicle access" [46]. NFPA itself has used the seven story assumption in publication [47].

http://dx.doi.org/10.1016/j.enbuild.2016.12.004
0378-7788/

of all U.S. HVAC energy consumption is used by pumps [10,11], but this likely significantly underestimates the requirements for large buildings and hydronic systems. A report by the U.S. Department of Energy's "Building America" program identified determining the electricity requirements for pumping in hydronic heating systems as a current research gap [12].

System complexity, the hydraulic response to highly variable loads, efficiency of individual pieces of equipment, interrelated effects of individual system components, and the tendency to apply large factors of safety in the design phase (i.e. oversizing equipment) all provide challenges to improving system energy performance, particularly in existing buildings [13,14].

This paper examines the energy effects of a suite of waterside retrofits in an urban high-rise mixed use (primarily residential) building's heating, cooling and DHW systems through analysis of extensive monitoring time series data. The paper first provides a review of recent research into the types of systems and equipment studied (Section 2). Section 3 describes the methodology, including study building description, experimental setup and analytical approach. Section 4 presents the pertinent results, and Section 5 discusses the implications of the paper's findings. In Section 6, conclusions from the current effort are offered, as well as needs for further research.

2. Background

Given publication space limitations, a detailed review of the systems and technologies investigated is not possible here; however, we provide a summary of research relevant to the effects studied.

2.1. Hydronic systems

Where dynamic hydronic systems for actual buildings have been analyzed, they have been limited to simple single-family residential construction [15] or models that have been evaluated without experimental validation [16,17]. The underlying theories of pipe network flow and pressure behavior and methods for solving them are well established [18]. These approaches have been extended to numerical models to solve the hydraulic equations associated with thermal hydronic networks as the system responds to loads changes [19–21]. A more integrated approach has also been studied in a laboratory setting in which the heat exchanger network acts as an emulator in a "hardware-in-the-loop" simulation, responding to the model and allowing for more tuning [22]. These studies have shown good agreement between predicted and actual performance; however, they have been limited to simplified laboratory heat exchanger networks for validation. There is a clear research gap for the evaluation of hydronic systems for actual large buildings.

2.2. Centrifugal pumps

The operating point of a hydronic system, defining the differential pressure, Δp, and the water flow rate, $\dot{V}$, is the intersection of the pump curve and the system curve. The pump efficiency, η_p, and to a lesser extent, the motor efficiency, η_m, also depend on this operating point. The system curve changes with load changes; however, the pump curve is fixed for a constant speed system.

The hydraulic power (commonly "water horsepower"), P_h, the pump power at the shaft (commonly "brake horsepower"), P_p, and the motor electric power, P_m, are related by:

$$P_m = \frac{P_p}{\eta_m} = \frac{P_h}{\eta_m \eta_p} = \frac{\dot{V}\Delta p}{\eta_m \eta_p} \quad (1)$$

This paper is primarily concerned with the electricity required to drive pumps. Selecting a pump for a new building requires estimating the pressure drop in the system under full load conditions. In estimating the zonal heating and cooling loads, a safety factor of at least 10% is typically applied, leading to larger terminal units [23]. Further, a building with many terminal units and/or proportional control valves is unlikely to ever be at the design load. Another safety factor is applied to the pressure drop after estimating losses at the design flow rate [24]. These safety factors and overestimates are compounded when determining the pump power required. The pump may be further oversized due to nominal equipment sizes and a pump size factor of safety. The result can be a far larger pump than needed for the actual system [25,26].

Pump oversizing can have significant impacts on energy performance throughout the hydronic system, including excessive pump motor electricity draw and low power factor, reduced heat transfer effectiveness of heating and cooling coils, and lower chiller efficiency [26,27].

Reducing the speed of the pump shaft can reduce the flow rate. The potential energy savings from this approach are exponential due to the pump affinity laws, relationships among water flow rate, $\dot{V}$, differential pressure, Δp, and pump power, P_p, at different rotational speeds, n_1 and n_2,:

$$\frac{\dot{V}_2}{\dot{V}_1} = \frac{n_2}{n_1}, \frac{\Delta p_2}{\Delta p_1} = \left(\frac{n_2}{n_1}\right)^2, \frac{P_{p,2}}{P_{p,1}} = \left(\frac{n_2}{n_1}\right)^3 \quad (2)$$

The affinity laws rely on the assumption that the pump efficiency does not change with speed and are generally accurate at the speeds seen in centrifugal pumps in building applications [28,29].

2.3. Variable frequency drives

The most common method of varying the speed of a pump is a variable frequency drive (VFD), which reduces the frequency of the electricity supply to an AC motor. The energy savings from VFDs can be overestimated [30], primarily because a small amount of electricity is needed to operate the VFD and the motor efficiency can decrease at reduced motor load/speed [31].

Previous studies of VFDs that identify deviations from the affinity laws focus on control schemes in existing variable flow systems rather than system design effects [17,32,33]. VFDs are typically controlled to maintain a differential pressure set point at some point hydraulically distant from the central plant equipment or across the main supply and return lines of the distribution loop, though more complex control strategies have been investigated to minimize energy usage or costs [32,34].

The benefits of VFDs for motors have been well documented for a wide range of applications [35], including several pumping applications: building heating and cooling systems [36,37], distributed heating systems [38] and industrial applications [39].

2.4. Flow control valves

Many types of valves are available for hydronic systems that offer a range of responsiveness to changes in system state and of control by building operators and BMS [40]. Flows through basic venturi valves and standard calibrated balancing valves can fluctuate widely during system operation. As loads fluctuate throughout a building, increased local pressures result in corresponding local flow increases. Pressure dependent control valves (PDCVs) can be adjusted (e.g. in response to a thermostatic sensor and control), but still respond with excessive flow to increased system pressure [41].

Pressure independent control valves (PICVs) offer the ability to control the flow rate set point through the BMS or local temperature sensor-control [42]. While manufacturers perform laboratory tests to determine valve accuracy and hysteresis effects, in-building energy effects of PICVs have not been studied.

3. Methodology

The research effort described in this paper included extensive monitoring of pre- and post-retrofit systems and analysis of analysis of the monitoring data to evaluate the effects of the HVAC modifications on system hydraulics and pumping electricity. Except where specifically noted, the approach to the chilled water (ChW) and hot water (HW) systems was identical.

3.1. Experimental setup

The study building is a 23-story mixed-use, primarily multifamily residential building with approximately 137,000 sq. ft. of occupiable floor space, located in Manhattan, New York, NY. Floors one and two are occupied by an array of commercial uses and the residential lobby; floors three through 21 contain 39 residential units and common hallways; and floors 22 and 23 house the building's central mechanical plant, elevators and other building equipment. The building is primarily clad in glazed curtain wall.

3.1.1. Original mechanical systems

The study building has a centralized hydronic system for heating, cooling and domestic water heating; the original HW system was constant-primary/constant-secondary (CPCS) and the original ChW system was constant primary only (CPO). The building's 22nd floor central plant, shown in Fig. 1, contains most of the hydronic system's central equipment: Two absorption chiller-heaters units capable of providing hot and chilled water (CH-1 and CH-2), two boilers (B-1 and B-2), three primary HW pumps circulating water through the chiller-heaters (P-10, P-11 and P-12), three primary HW pumps circulating water through the boilers (P-13, P-14 and P-15), five distribution pumps (P-1 through P-5), and three condenser water pumps (P-6, P-7 and P-8) circulating water between the chiller-heaters and cooling towers on a roof one story above (CT-1 and CT-2).

The HW system includes three secondary loops: One space heating hot water (HW-SH) loop and two HW loops feeding the internal coils of storage water heaters (these hot water flows are designated "HW-DHW"). Two dedicated pumps (P-4 and P-5) draw HW from the primary loop and can circulate water through any of the secondary HW loops. HW-SH is distributed to 181 FCUs and nine AHUs through a reverse return distribution system of eight risers. HW Flow to each AHU is controlled by a modulating valve or a two-way valve. The HW-DHW is distributed to two storage water heaters serving the upper half of the building and two storage water heaters serving the lower half of the building.

Two dedicated pumps (P-1 and P-2) circulate ChW through the chiller-heaters and, through a reverse return distribution system parallel to that of the HW-SH secondary loop, to 181 FCUs and 12 AHUs. ChW flows at terminal units are controlled in the same manner as HW-SH flows. P-3 and serve any of the secondary loops.

Appendix Table A1 summarizes relevant AHU information. Appendix Table A2 summarizes relevant central plant pump information.

3.1.2. Retrofit description

A retrofit of the original mechanical system was completed between February 17 and September 16, 2015. The retrofit of the central plant is shown in Fig. 2 and included the following scope:

3.1.2.1. Chilled water primary/secondary. ChW piping was modified to separate the ChW system into a primary loop and a secondary loop. Two new pumps were installed with P-16 and P-17 circulating ChW through CH-1 and CH-2, respectively.

3.1.2.2. Pump replacement. All existing central plant pumps were replaced with smaller and/or more efficient pumps. In the new arrangement, P-4 is dedicated to HW-SH and P-5 is dedicated to HW-DHW.

3.1.2.3. Variable frequency drives. VFDs were installed on all secondary loop pumps (P-1 through P-5). The speed of ChW pumps P-1 and P-2 is controlled to maintain a set point pressure differential across a hydraulically distant point on the basement level. The speed of HW-SH pump P-4 is similarly controlled to maintain a set point pressure differential across a point on the HW loop. The speed of HW-DHW pump P-5 is controlled to maintain a set point pressure differential in the lower zone DHW room on the basement level.

3.1.2.4. Air handling unit pressure independent control valves. PICVs were installed on the hot and chilled water lines of AHUs 1 through 5. A limited selection of AHUs was used to be able to install and control the new ChW PICVs in parallel to the existing control valves within the project budget. These five AHUs' total design water flow rate represent 28% of the building's total design ChW flow rate (and 23% of the total design cooling load). It is expected that during times of the year when the building's cooling load is low (e.g. in the winter), these percentages will be higher because some of these AHUs will be in use throughout the year whereas the residential FCUs are unlikely to be.

3.1.2.5. Domestic hot water pressure independent control valves. PICVs were installed on the HW-DHW intake lines at each DHW storage water heater and controlled to call for HW-DHW when the potable DHW water send temperature fell below a set point.

3.1.3. System monitoring

The sensors and related equipment used were limited to existing chiller plant sensors and noninvasive equipment. All data was logged at one-minute intervals and accessed through a new building management system (BMS).

Ultrasonic flow meters were installed to measure the volumetric flow rate of (1) the ChW distribution/secondary loop supply and (2) the HW-SH secondary loop supply.

The differential pressure (Δp) was measured (1) across the pump assembly of P-1 through P-5, (2) between the supply and return of the ChW and HW-SH distribution loops, and (3) across the ChW coils of AHUs 1 through 3. An ultrasonic flow meter was installed temporarily at each of the three AHUs for which differential pressure measurements were continuously monitored (Item 3 in the previous sentence); a manual balancing valve was adjusted and the resulting flow-pressure relationships were used to estimate the water flow rate using continuous Δp monitoring data.

Existing thermistors were used to monitor the temperature of (1) the supply and return of the ChW and HW-SH distribution loops and (2) various points in the central plant. In addition, surface-mounted thermocouples were installed at the ChW supply and return of AHUs 1 through 3.

The ChW valve control signals at AHUs 1 through 3 were integrated into the new BMS and logged.

The electricity draw was measured at the three-phase electrical supply to P-1 through P-5. In the post-retrofit monitoring, these electricity measurements included the VFD for each of the five pumps.

During the post-retrofit monitoring phase, the ChW system was operated in four states by setting the VFD to auto or bypass (i.e. 100% pump speed). The modified system is able to operate with either the original PDCVs or the new PICVs at the subset of five AHUs at which the PICVs were installed. Table 1 describes each post-retrofit state.

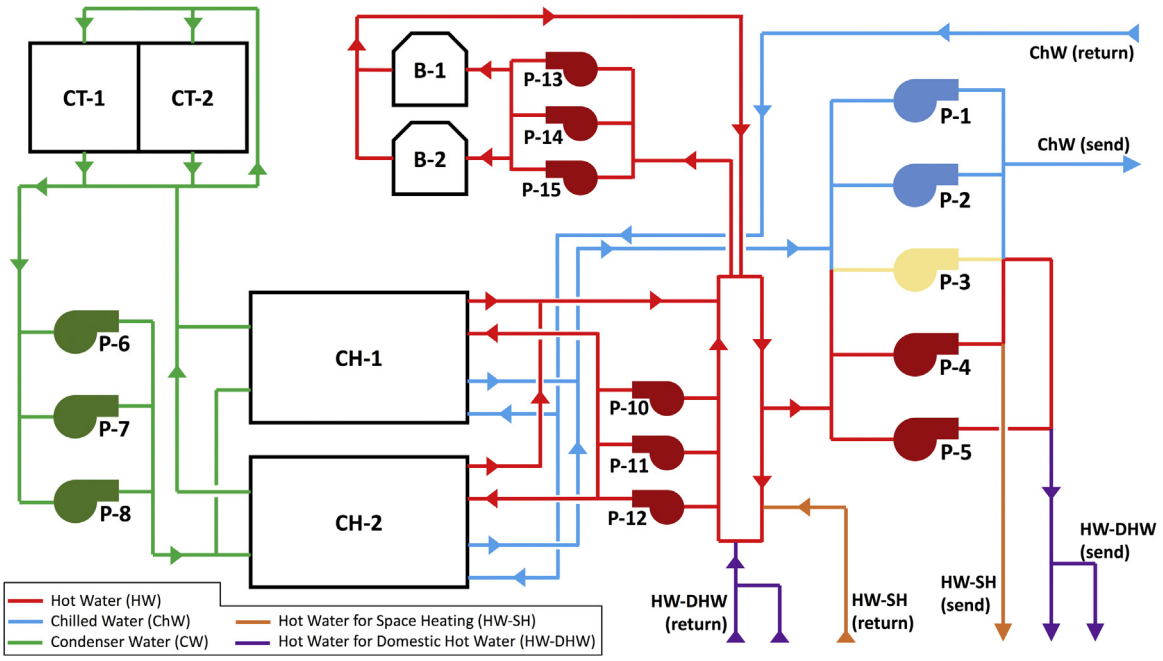

Fig. 1. Schematic of original central mechanical plant equipment, pumps and water flows.

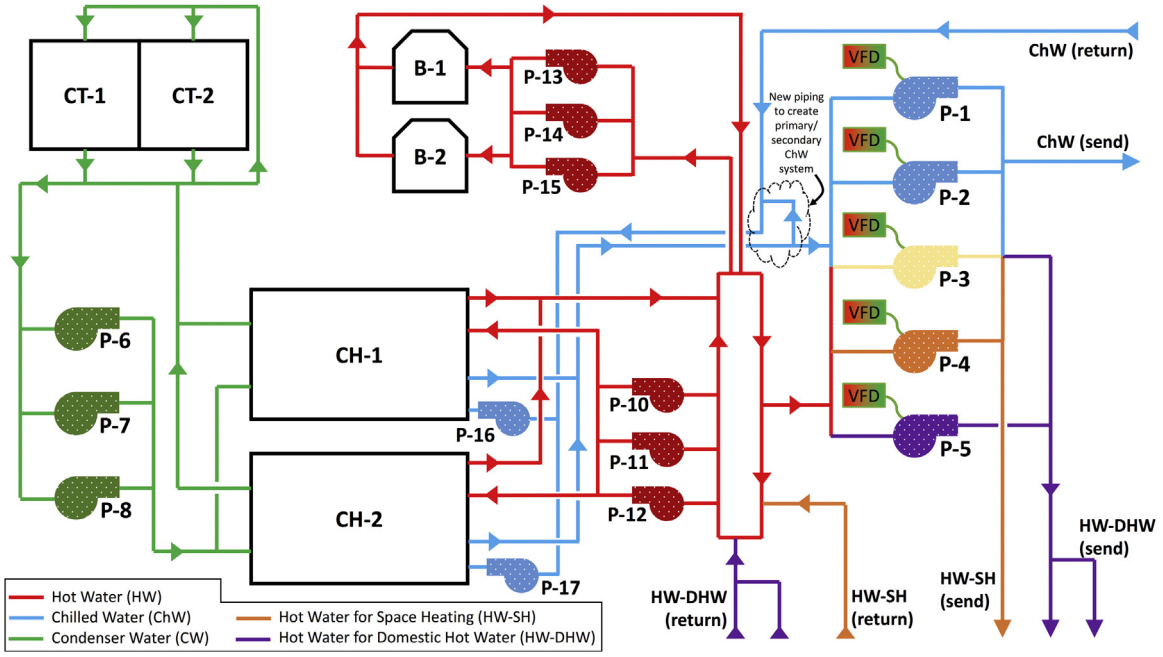

Fig. 2. Schematic of post-retrofit central mechanical plant equipment, pumps and water flows. Hatch patterns indicate new pumps. Clouded area indicates new piping to create chilled water primary loop.

Table 1
Chilled water operating states during monitoring.

Scenario	Pump	VFD	AHU Subset Valves
Pre-Retrofit	Original	N/A	Original
State A	Replacement	Auto	PICVs
State B	Replacement	Auto	Original
State C	Replacement	Bypass	PICVs
State D	Replacement	Bypass	Original

3.2. Analysis

The time-varying building thermal load was used as a benchmark for comparing the distribution energy in the post-retrofit states and the pre-retrofit state. The thermal load (i.e. heating or cooling load) is computed from the water volumetric flow rate, $\dot{V}$; the difference between water distribution loop return temperate, T_r, and supply temperature, T_s; and the water's density, ρ, and specific heat, c_p. The load cannot be calculated at a given one-minute time step, t, due to the time required for water to pass through the hydronic system. An earlier study found that uncertainty in thermal response of hydronic systems approaches zero at one-hour

time steps [43]. As such, the hourly load, $\dot{Q}_h$, is calculated over the number of time steps, τ_h, in the hour, h:

$$\dot{Q}_h = \begin{cases} \frac{1}{\tau_h}\sum_{t\in h}\rho c_p \dot{V}_{z,t}(T_{z,r,t} - T_{z,s,t}), \text{ z = ChW} \\ \frac{1}{\tau_h}\sum_{t\in h}\rho c_p \dot{V}_{z,t}(T_{z,s,t} - T_{z,r,t}), \text{ z = HW-SH} \end{cases} \quad (3)$$

Similarly, the average electric power draw of the distribution pumps was computed for each hour, $P_{dist,h}$, from the measured power draw, $P_{dist,t}$:

$$P_{dist,h} = \frac{1}{\tau_h}\sum_{t\in h} P_{dist,t} \quad (4)$$

In Eqs. (3) and (4), τ_h is not necessarily 60 min due to some data gaps; only hours with at least 31 min of data were used for these computations and related analyses.

While the actual pump power at specific loads in the time series can be compared directly from the monitoring data and Eqs. (3) and (4), the total annual pumping electricity for each scenario to meet all loads is desired. This presents two separate problems:

1 Determining the electricity required to operate the pumps at other times when the load is within the ranges captured in the monitoring periods.
2 Projecting the electricity required to operate the pumps at higher loads than those captured in the monitoring periods.

The maximum thermal load in the monitoring periods, delineating the boundary between these two approaches, is defined as the transition point, $\dot{Q}_{TP}$.

3.2.1. Estimating pump power at thermal loads within monitoring range

A statistical approach, based on the behavior of hydronic systems, was used to approximate general relationships for pump power vs. load for loads within the ranges captured in the monitoring periods. For constant speed operation, differential pressure across the pump (head), Δp_{pump}, is related to water flow rate, $\dot{V}$, by the following general formulation, where c_1 and c_2 are some system-specific constant coefficients:

$$\Delta p_{pump} = c_1 - c_2\dot{V}^2 \quad (5)$$

Though the thermal load is not perfectly proportional to the water flow rate, the relationship in Eq. (6) was found to provide a satisfactory fit to the data for the pre-retrofit pump and post-retrofit States C and D:

$$P_{dist,const} = \alpha_1 + \alpha_2\dot{Q}_h - \alpha_3\dot{Q}_h^3 \quad (6)$$

where $\alpha = (\alpha_1, \alpha_2, \alpha_3)$ is a vector of constant coefficients determined by linear regression using the base statistical package in R [44].

With the VFD in operation, differential pressure across the pump (head), Δp_{pump}, is related to water flow rate, $\dot{V}$, by the following, where c_1 and c_2 are some system-specific constant coefficients[2]:

$$\Delta p_{pump} = c_1 + c_2\dot{V}^2 \quad (7)$$

With the same assumption that water flow rate is closely correlated with load and allowing for efficiency effects, including the electricity required to operate the VFD itself, the following relationship was used for post-retrofit States A and B:

$$P_{ChW,dist,var} = \beta_1 + \beta_2\dot{Q}_h + \beta_3\dot{Q}_h^3 \quad (8)$$

where $\beta = (\beta_1, \beta_2, \beta_3)$ is a vector of constant coefficients determined by linear regression using the base statistical package in R.

3.2.2. Estimating pump power at loads beyond monitoring range

The pump power consumption for higher loads, outside the range captured in the monitoring periods, is necessary to characterize the annual operation of the system. A two-step approach is used:

1 The hydraulic behavior (flow-pressure relationship) of the system is projected at higher loads.
2 The pumping electricity required to serve the hydraulic system characteristics identified in Step 1 are computed.

The general equation for a hydronic system curve is given by the following:

$$\Delta p = k\dot{V}^2 \quad (9)$$

The characteristic constant of the system curve, k, is correlated to load changes as valves in the system open, close and modulate. Because the system hydraulics can change rapidly, it was necessary to investigate system curve changes at the highest time resolution possible, the one minute time step at which data was recorded.

The system curve constant generally decreases with increasing load; however, this behavior is both non-linear and is influenced by the distribution of loads in the system. The variation of system curve constant in response to the system load, $\dot{Q}$, can be shown to have an upper bound, k_{upper}, and a lower bound, k_{lower}, as functions of the system load.

$$k_{upper} = c_1 + \frac{1}{(c_2 + c_3\dot{Q})^2} \quad (10)$$

$$k_{lower} = c_4 + \frac{1}{(c_5 + c_6\dot{Q})} \quad (11)$$

where $c_1, \ldots, c_6$ are some system-specific constants.

In general, these bounds are not likely to be observed in real systems: The upper bound represents a perfectly distributed load (i.e. all terminal units having the same load) and the lower bound represents a perfectly concentrated load (i.e. the full building load in a single terminal unit). The two curves approach each other as the thermal load approaches zero (i.e. all valves closed) and as the load approaches the maximum (i.e. all valves open).

3.2.2.1. Projecting system hydraulic behavior. To project the hydraulic behavior of the system, the upper bound and lower bound functions were estimated for the pre-retrofit system and each of the post-retrofit states by nonlinear regression of the monitoring data. System hydraulic behavior was analyzed at one-minute time steps; however, due to the previously noted uncertainty in the thermal load at such high resolution, subsets of k-value data were used to estimate Eqs. 9 and 10. The computed loads were allocated to bins in 5 kW increments. The upper 5% of k-values in each bin was used to fit Eq. (10), and the lower 5% of k-values was used to fit Eq. (11). Only time steps with loads above 100 kW were used because (1) k-values near the upper bound are not expected at low loads and (2) the only system behavior projections needed were for cooling loads above 371 kW and space heating loads above 555 kW.

3.2.2.2. Projecting pump power. To compute the estimated pump power at the projected loads, relationships between pump power and k-value were necessary. While the hydraulic system behavior

[2] This relationship does not apply when the VFD operates at its minimum frequency (30% pump speed) as the differential pressure at the VFD pressure sensor exceeds the set point.

is affected by the presence of PICVs, the pump itself responds to the overall system pressure differential. As such, for the purposes of determining the relationship between pump power and k-value, the constant speed post-retrofit states (C and D) can be grouped together and the variable speed post-retrofit states (A and B) can be grouped together.[3]

A statistical approach was used to estimate the pump power at low k-values. For all scenarios, the projected values of k are less than 10^{-4} (and generally significantly lower) for the projected loads; therefore, only time steps with k-values less than 10^{-4} were used in developing functions to project pump power. A general decreasing exponential function was used for constant speed pump power, $P_{pump,const}$, as a function of k:

$$P_{pump,const} = \delta * e^{-m*k} \quad (12)$$

where δ and m are the constants found through nonlinear regression.

Although fitting Eq. (12) to the data is a purely statistical approach, the results of the nonlinear regressions show good agreement with the data and little deviation from the trends seen in the load range covered by the pre- and post-retrofit monitoring periods.

For each pre- and post-retrofit state, x, a function for the projected k-value, $k_{proj,x}$, is used to compute the projected pump power, $P_{dist,proj,x}(k_{proj,x})$, by Eq. (12). A weighting factor, r_x, that relates $k_{proj,x}$ to $k_{lower,x}$ and $k_{upper,x}$ is computed for each state such that the pump power draw at the transition point thermal load, $\dot{Q}_{TP}$, is continuous when using the function for projected pump power and using Eq. (6) or (8) per the analysis described in Section 3.2.1.:

$$k_{proj,x} = r_x k_{upper,x} + (1 - r_x) k_{lower,x} \quad (13)$$

such that:

$$P_{pump,const} = \Delta * e^{-m*k} \quad (14)$$

4. Results

After monitoring the pre- and post-retrofit systems described in Section 3.1, the chilled water and hot water systems were analyzed per Section 3.2.

4.1. Chilled water

Fig. 3 shows the hourly cooling load time series over the complete monitoring period, from September 2014 to February 2016. The expected seasonal variation is clear with the peak of 718 kW in the summer (July 29, 2015 at 4pm) and the minimum of 12.7 kW in the winter (January 23, 2016 at 5pm). Fig. 3 includes a line showing the smoothed conditional mean of the time series computed using a general additive model via the R package "ggplot2" [45].

Due to the timing of the monitoring equipment installation and the retrofit, no pre- or post-retrofit monitoring occurred in the peak cooling season (mid-summer). The maximum cooling loads recorded pre-retrofit and post-retrofit were approximately 400 kW and 450 kW, respectively. The post-retrofit building operated in the four states described in Table 1.

A cumulative distribution of the cooling loads observed during the one-year period from September 1, 2014 to August 31, 2015 is shown in Fig. 4(a); the cooling load distribution indicates that most cooling loads are significantly less than the peak cooling load. The maximum cooling load captured for the pre-retrofit period and all post-retrofit states was 371 kW. Cooling loads less than or equal to 371 kW constitute more than 84% of the full cooling load time series shown in Fig. 3. The effect of this limitation on the cumulative distribution of cooling loads is shown in Fig. 4(b) for each state.

4.1.1. System hydraulics

The chilled water flow rate in the secondary loop varies significantly with load and is highly dependent on the system configuration state, as shown in Fig. 5. With the VFDs in operation (States A and B), the chilled water flow rate generally reduces to less than 40% of the water flow rate required to meet the same hourly cooling load with the pump operating at a constant speed (States C and D).

The differential pressure of the pump varies with the water flow rate as seen in Fig. 6. For constant speed operation, the pressure follows an approximately inverse quadratic relationship with the water flow rate. The pressure differential with VFDs in operation is significantly lower and increases with increasing water flow rate according to an approximately quadratic relationship. The difference between the pump curves of the pre-retrofit and post-retrofit pumps is due to the reduction in pump size.

4.1.2. Air handling units

The AHUs were monitored and analyzed to evaluate the PICV effects. Comparing the constant speed pump scenarios using Fig. 7, the linear trend of flow vs. valve opening of the PICV (State C) is clear and the excessive flow of the existing pressure-dependent valves (State D) is eliminated. With the VFD in operation, the resulting lower system pressure causes lower local water flow rates. Below 60% valve opening, the flow with the existing valve (State B) is very low and does not vary with the signal. The PICV's mechanical response to differential pressure (State A) allows flow to the AHU before plateauing when the system pressure is no longer sufficient to maintain the needed pressure differential across the PICV. At valve opening signals above approximately 75%, the AHU flow is the same with and without PICVs.

For the more simple two-way valve at AHU-3, Fig. 8 shows the cooling coil water temperature differential improves with PICVs in both constant speed pump operation (State C vs. State D) and variable speed pump operation (State A vs. State B). A higher water temperature differential at a particular cooling load indicates higher heat transfer efficiency. As the AHU-3 valve does not have modulating control between fully open and fully closed positions, the relationship between temperature differential and load for each state was used to compare the pressure-independent mechanical response of the PICV to the pressure-dependent response of the original valve. The higher temperature differential for the PICV scenarios for cases both with and without VFDs in operation indicates improved efficiency of the AHU.

4.1.3. Distribution/secondary pump power

The variable speed scenarios (States A and B) require significantly less electricity to operate the pumps than the constant speed scenarios ("Pre-Retrofit" and States C and D). This effect can be seen in Fig. 9, which shows the hourly average pump electric power vs. hourly average cooling load. Though more modest than the VFD effects, electricity usage of the smaller replacement pump is clearly lower than that of the larger original pump.

"PICV" indicates PICVs on 28% of the building's total design ChW flow rate.

To project pump power beyond the cooling load range for which monitoring data was collected, the hydraulic system behavior for each state was first projected as described in Section 3.2.2.1. The pump power required to circulate flow in these projected system configurations was then computer as described in Section 3.2.2.2.

Fig. 10 shows the overall functions of chilled water distribution pumping power for each scenario. As in the initial analysis of the

[3] This applies only to the ChW system; all post-retrofit HW scenarios include the PICVs.

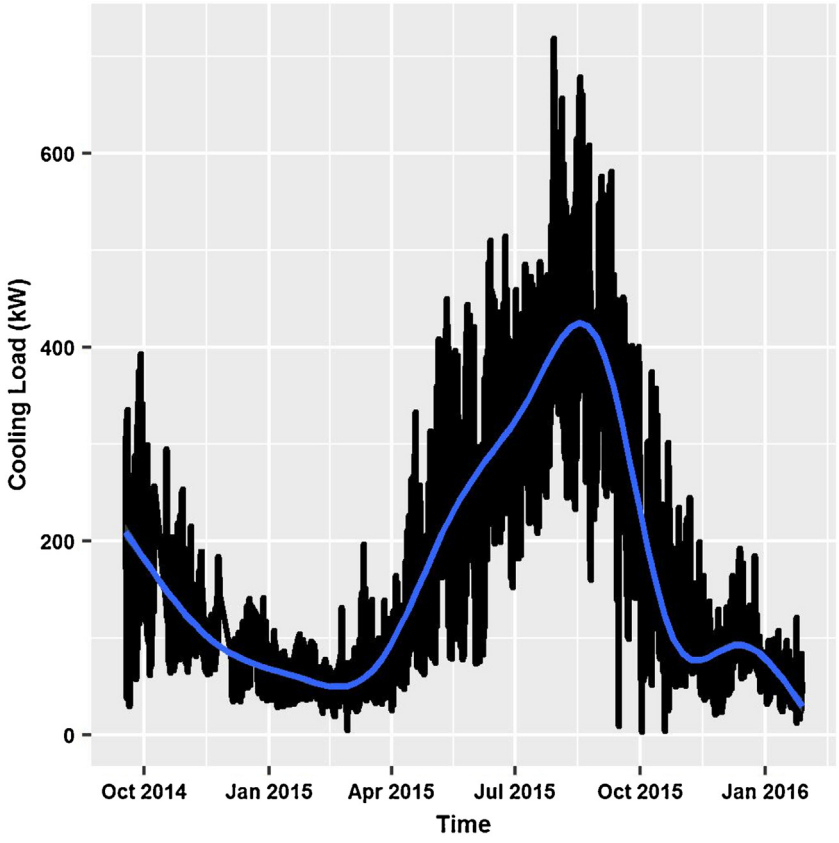

Fig. 3. Hourly cooling load time series.

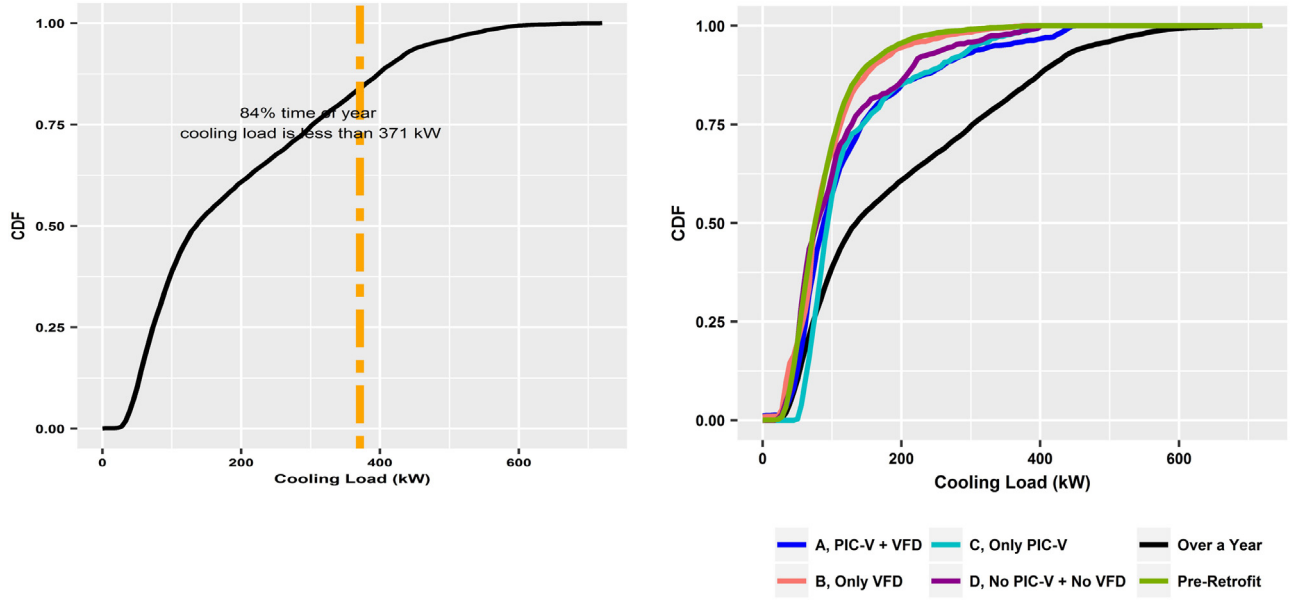

Fig. 4. Cumulative distribution of hourly cooling loads for (a) the full time period September 2014–August 2015 and (b) different states of operation and system configuration. Vertical line indicates maximum cooling load in pre- and post-retrofit monitoring periods.

monitoring data (Fig. 7), the effect of the replacement pump (State D vs. Pre-Retrofit) is clear. The PICVs further reduce pumping power (State C vs. State D); the larger effect at high cooling loads is likely due to the PICV limiting AHU water flow with constant speed pump operation. The VFDs have the most significant effect of all interventions (States A and B), with the most pronounced impact in the midrange cooling loads. The crossing of projections for States A and B at approximately 450 kW cooling load could be explained by the PICV allowing more water flow (though still below the design flow) with the VFDs in operation than the existing control valve at high cooling loads; at lower cooling loads, which occur much more frequently, the pumping power is slightly less with PICVs (State A) than without (State B).

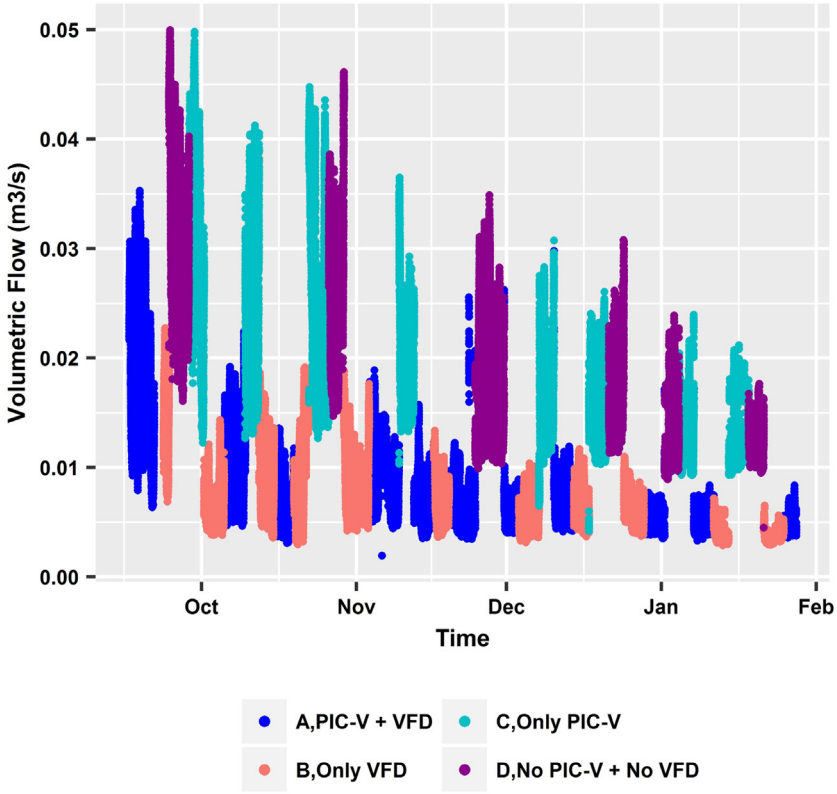

Fig. 5. Post-retrofit chilled water flow in the secondary loop with states indicated.

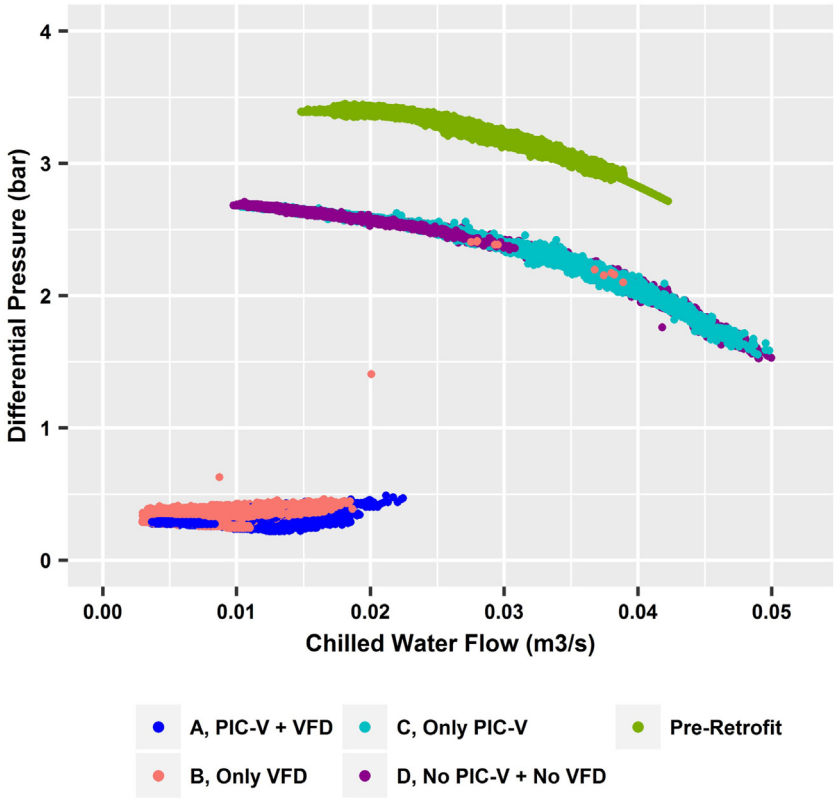

Fig. 6. Differential pressure of pump with varying water flow rate; each state indicated.

The purpose of the pump power projection method described in Section 3.2.2 was to estimate expected values from the regression approach of Section 3.2.1 had monitoring data been available for the full range of cooling loads. As such, the total distribution pumping

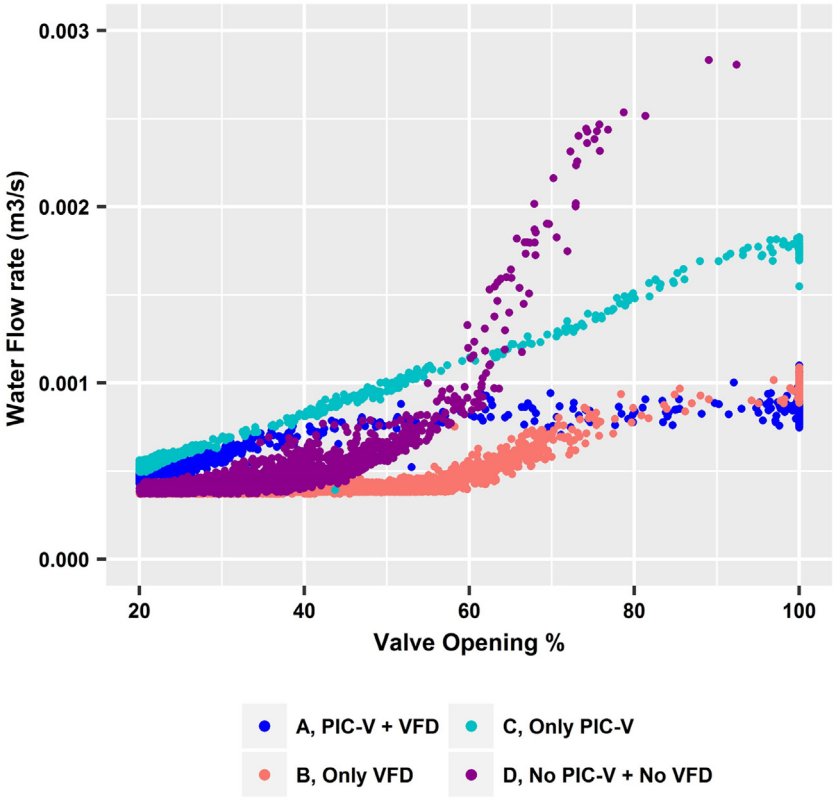

Fig. 7. AHU-1 chilled water flow rate vs. valve opening%.

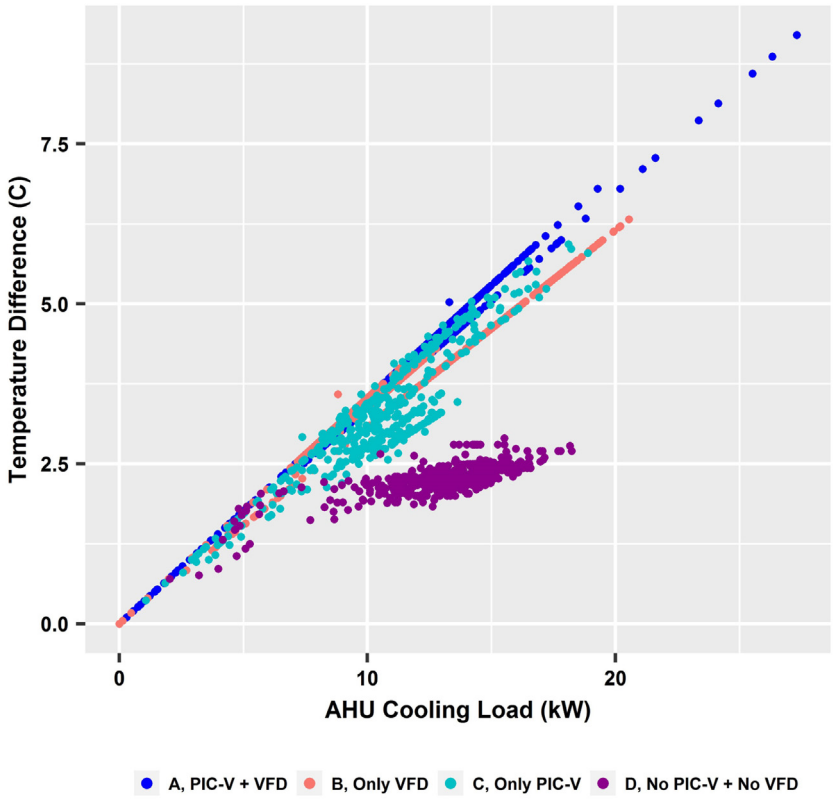

Fig. 8. AHU-3 cooling coil temperature differential vs. AHU cooling load.

energy to meet cooling loads between 300 kW and 371 kW was projected using the monitoring data from cooling loads less than 300 kW and the methodology of Section 3.2.2 and compared to the regression fit. For this cooling load range, the difference in the total

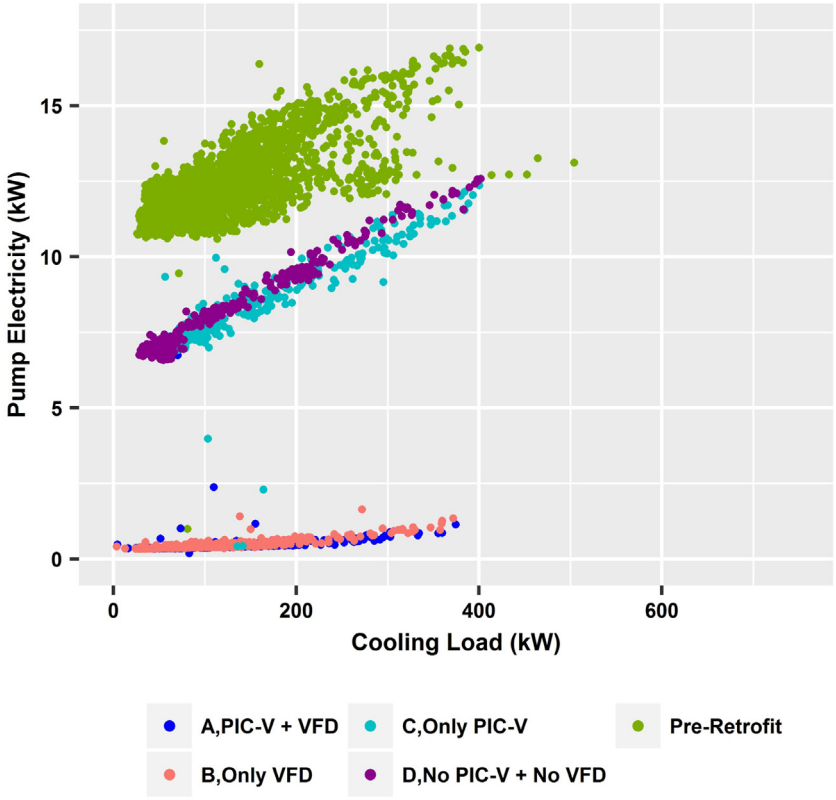

Fig. 9. Chilled water secondary/distribution loop hourly average pump power vs. hourly average cooling load.

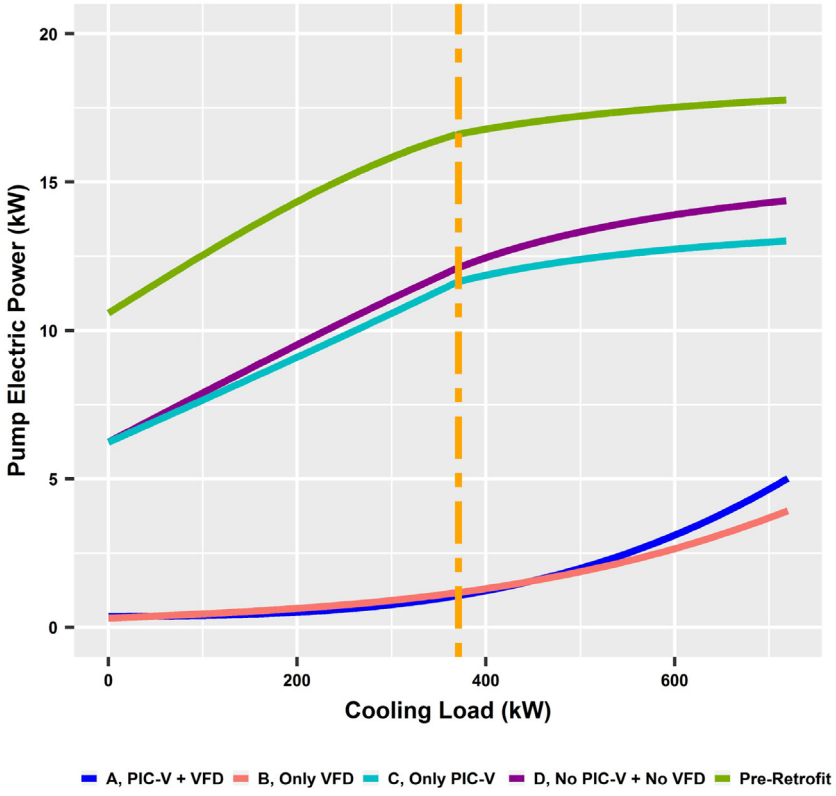

Fig. 10. Average hourly pump electric power draw estimates vs. cooling load. "PICV" indicates PICVs on 28% of the building's total design ChW flow rate.

pumping energy computed using the two approaches was within 1.6% for all states using this approach.

4.1.4. Annual cooling system pumping energy

For each state, the expected distribution pumping power was computed for each time step over the course of the study year

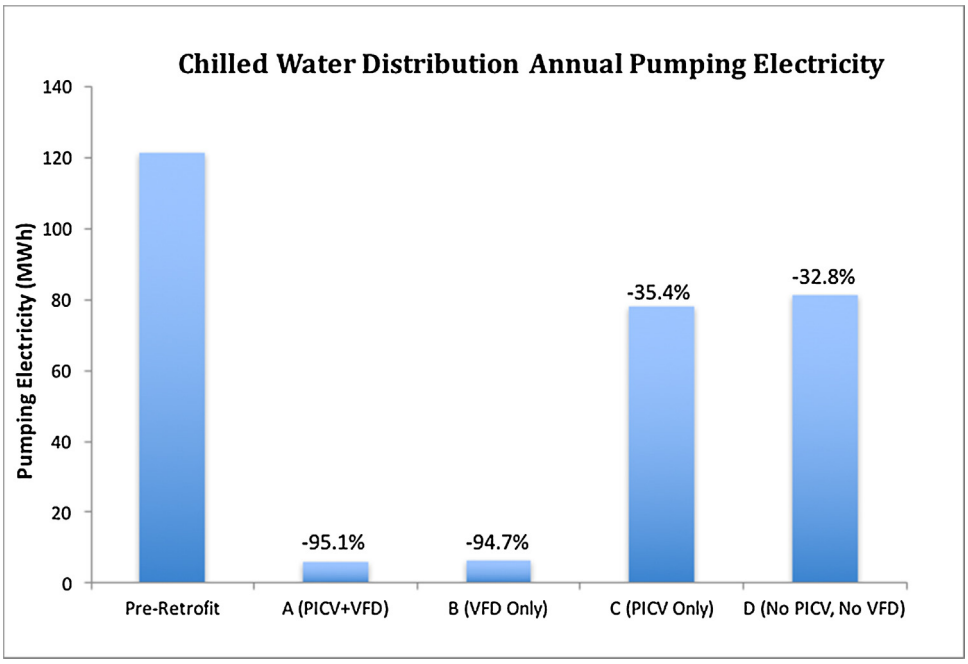

Fig. 11. Total annual secondary/distribution chilled water pumping energy.

using the appropriate approach from Section 3.2. The power values at each minute were then aggregated to compute the annual pumping energy required for each scenario; Fig. 11 shows these results. The annual calculations show very significant reductions in energy usage due to both the replacement pumps and the VFDs; the impact of the PICVs is also discernable, particularly in the case with constant speed pumping.

4.1.4.1. Percentages shown represent annual energy savings compared to the pre-retrofit energy requirements. "PICV" indicates PICVs on 28% of the building's total design ChW flow rate. The power draw of the new constant speed, constant flow primary pumps necessitated by the change to a CPVS arrangement was assumed to be constant. This was confirmed by "spot" measurements made approximately biweekly during the post-retrofit period using a handheld Fluke multimeter. The average power draw of the primary ChW pump was 6.3 kW with all values within +/−1.2% of the mean.

The power draw of the constant speed, constant flow was also assumed to be constant in the pre- and post-retrofit periods. This was confirmed by spot measurements made approximately biweekly during both the pre- and post-retrofit periods. The mean power draw of the original CW pump was 25.3 kW with all values within 0.5% of the mean; the mean power draw of the replacement CW pump was 18.0 kW with all values within 0.7% of the mean. The CW pumps are the dominant pumping energy demand, and their reduction in energy use contributes more to overall energy savings than the combined effects of the CPVS pumps. With all retrofits considered, the total annual cooling pumping energy reduction was computed to be 36% compared to the original system.

4.2. Hot water system

The hot water system, as analyzed here, includes the primary hot water loop, the secondary hot water loop for space heating (HW-SH), and the secondary hot water loop for domestic hot water (HW-DHW). The post-retrofit HW system did not have the same functionality allowing various post-retrofit states as in the ChW system.

Fig. 12 shows the space heating load time series over the complete monitoring period, from September 2014 to February 2016. The expected seasonal variation is clear with the peak of 691 kW in the winter (January 8, 2015 at 6am) and the minimum of 9 kW in the summer (June 10, 2015 at 1pm).

4.2.1. Hot water distribution pumping

With the oversized original pumps in place during the pre-retrofit period, P-5 served both the secondary HW-SH and HW-DHW loops. In the post-retrofit period, separate pumps serve the HW-SH secondary loop (P-4) and the HW-DHW secondary loop (P-5). Fig. 13 shows the hourly pump power for the pump serving the space heating load vs. the hourly space heating load. A very significant reduction in pumping power is observed, with the variable speed pump power steadily increasing with increasing space heating load.

4.2.1.1. Pre-retrofit pump serves both HW-SH and HW-DHW. Although both the pre-retrofit and post-retrofit monitoring periods captured the peak winter heating condition, lower space heating demands due to higher winter temperatures during winter 2015–2016 resulted in a peak space heating demand of 555 kW (compared to 691 kW during the September 2014 to August 2015 period of interest for annual energy calculations). The pump power projection approach described in Section 3.2 was employed to project pump power requirements for the post-retrofit space heating loads between the 555 kW peak post-retrofit space heating load and the 691 kW peak overall space heating load. The dominance of the VFD effects on energy savings remains clear as the heating load increases; however, the replacement pumps likely remain significantly oversized as the electric power draw of P-4 remains low throughout the space heating load range.

The electric power draw of the HW-DHW post-retrofit pump (P-5) fluctuates as the PICVs respond to the thermostat control described in Section 3.1.2. Due to a lack of existing temperature sensor taps on the HW-DHW loops, it was not possible to develop thermal load time series for the two HW-DHW loops as was done for the ChW and HW-SH distribution loops. However, no discernable seasonal or diurnal patterns were observed in the pump power

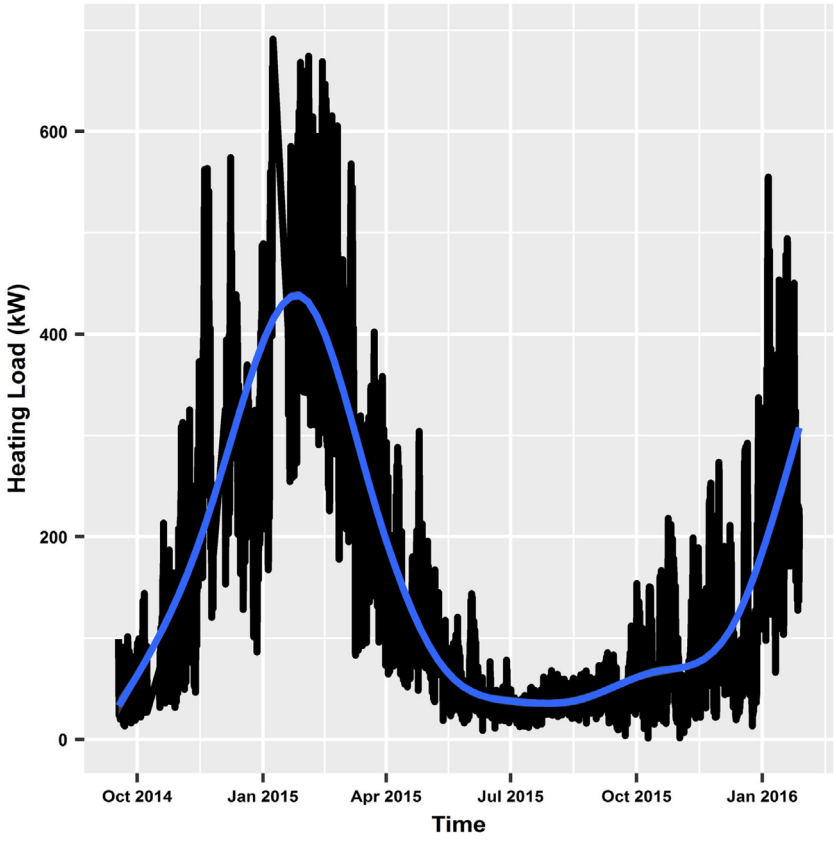

Fig. 12. Hourly space heating load time series.

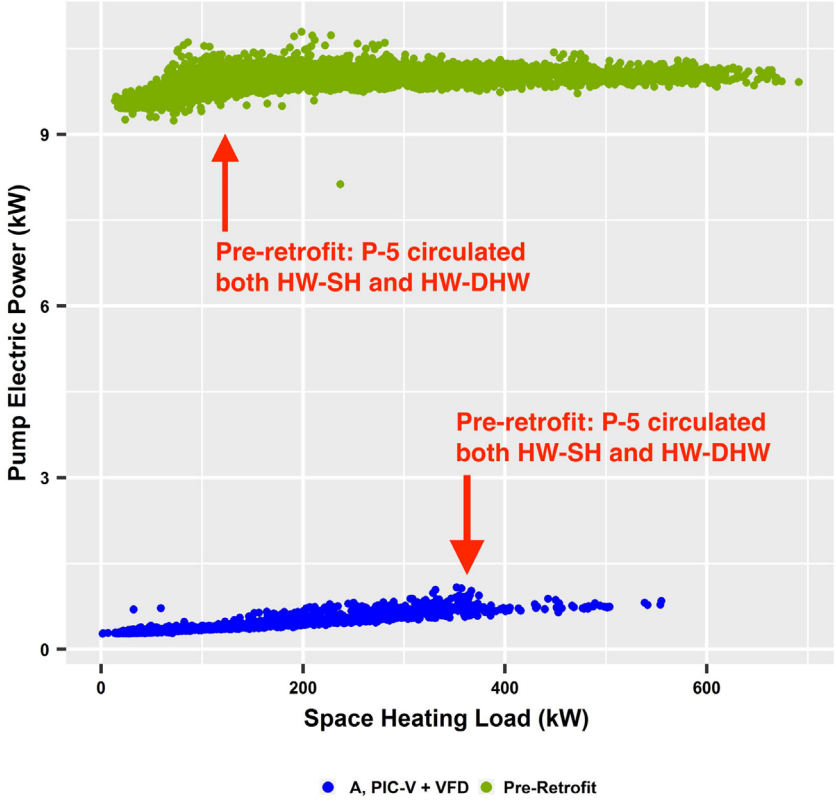

Fig. 13. Average hourly distribution/secondary loop pump electric power for space heating hot water distribution.

draw to serve these loads. As such, the average electric power draw of P-5, 0.84 kW, was used in computing the total annual electricity for secondary HW pumping. The total annual secondary HW pumping energy reduction (85%) is less than that of the ChW system; this is primarily due to the use of two secondary HW pumps in the post-retrofit HW system compared to one secondary pump in the pre-retrofit HW system and in the ChW system.

The power draw of the constant speed/constant flow primary HW pumps was assumed to be constant. The average power draw of approximately biweekly spot measurements of the original chiller-heater HW pump (either P-11 or P-12) was 6.6 kW with all values within 3.1% of the mean; the average power draw of the replacement chiller-heater HW pump was 7.0 kW with all values within 2.2% of the mean. In the pre-retrofit period, all three boiler HW pumps (P-13, P-14 and P-15) operated with average power draw of 2.0 kW, 1.7 kW and 1.6 kW; all readings were within 3.3%, 2.7% and 4.2%, respectively, of these values. The average power draw of the single replacement boiler HW pump that operated in the post-retrofit period was 2.5 kW with all values recorded at this value. Therefore, the total pre-retrofit primary HW pump electricity draw was assumed to be a constant 11.9 kW and the total post-retrofit primary HW pump electricity draw was assumed to be a constant 9.5 kW.

4.3. Total central plant pumping energy

All central plant pumping energy was aggregated for the pre- and post-retrofit (ChW State A) conditions. Fig. 14 shows the 41% reduction in total central plant pumping energy. The largest contributors to the energy reduction are the pumping electricity savings from, in order: (1) Secondary/distribution ChW, (2) secondary HW, (3) condenser water, and (4) primary HW. (All values represented in Fig. 14 are included in Appendix Table A3)

The total annual central plant pumping energy of the original system, 537 MWh, represents 55.4% of the 967 MWh total owner-metered electricity during the year of interest. The 221 MWh decrease in the post-retrofit system's electricity usage reduces the total owner-metered electricity usage by 22.8%. Using the building's current blended electricity price of $161.5 per MWh, the annual owner-metered natural gas usage of 12,974 GJ (123,000 therms) and the building's current natural gas price of $10.71/GJ ($1.13 per therm), the approximately $36,000 reduction in annual central plant pumping electricity costs represents a 12.1% reduction in all owner-paid energy costs for the building.

5. Discussion

To date, variable flow control in hydronic HVAC systems has been more focused on commercial buildings than on residential buildings. However, multifamily buildings dominate the current growth in U.S. building floor area with increased concentration in large buildings. Further, increased urbanization and the prevalence of mixed use buildings in dense urban areas warrants increased focus on this building type.

Individual energy conservation technologies generally are part of larger integrated building systems; oftentimes, they exhibit energy savings at part-load operation, when the actual system loads are not at their peak conditions. Evaluating these technologies within operating systems can give a better understanding of their effects on overall building energy usage than can standard laboratory efficiency tests. Of particular interest are buildings with highly variable cooling and heating loads that maintain a relatively low level of constant year-round demand.

In this study, the performance of hydronic heating and cooling distribution systems typical of those found in urban mixed use, multifamily residential buildings were investigated and the impact of a suite of energy conservation measures (ECMs) on those systems was evaluated. In the original building, the central plant pumping equipment was found to be responsible for 55% of total annual owner-metered electricity usage and 29% of all annual owner-paid utility bills (including electricity and natural gas charges).

Oversized pumps were found to cause unnecessarily high pressure differentials and flow rates in the system. At the AHUs for which detailed monitoring was performed, excessive flow and low temperature differentials ("low ΔT") were observed across the coils, implying potential for both system-wide component degradation and low heat transfer efficiency at the terminal units.

The use of pressure-independent control valves (PICVs), which respond to pressure changes in the system to maintain the desired water flow at terminal units, eliminated overflow conditions and improved ΔT at the monitored AHUs. Only a subset of terminal units, representing 28% of the building's peak design ChW flow, was outfitted with PICVs in the post-retrofit monitoring period. The use of PICVs in these units exhibited small yet significant reductions in annual secondary pumping electricity estimates (4%) compared to the post-retrofit constant speed pump operation without PICVs. Similar improvements in flow control and ΔT would be likely if PICVs were to be installed at additional units; however, the energy effects cannot be extrapolated to a scenario of full PICV deployment given the highly nonlinear response within a complex system.

When used in conjunction with VFDs, the opposite water flow effects were observed at the major AHUs compared to the constant speed pump scenarios: With VFDs in operation, the original control valves were unable to provide the necessary water flow rate at all valve settings. While the PICVs also provided lower-than-design flows at higher valve open settings, water flow rates were significantly higher than for the original valves at low and midrange valve settings.

The pumping electricity reduction with VFDs was far more significant than the effects of other ECMs: Annual replacement ChW distribution pump electricity was 92% lower with VFDs than without. When comparing the combined effects of the replacement pumps and the VFDs, the ChW distribution pumping electricity reduction was 95%. At the low cooling loads that dominate the building system's demand profile, the PICVs further reduced pumping electricity requirements. In aggregate, though the total annual electricity usage was also very low in the replacement pump-VFD scenario (6.4 MWh), the replacement pump-VFD-PICV scenario needs slightly less annual electricity (6.0 MWh).

Although less detailed monitoring was performed on the hot water (HW) secondary loops for space heating (HW-SH) and domestic hot water (HW-DHW) than on the ChW system, similar results were observed. The overall ECM package (replacement pumps, VFDs, and PICVs at select AHUs and all DHW storage water heaters) resulted in an estimated annual pumping electricity savings of 85%, despite the need for two secondary loop pumps (one for HW-SH and one for HW-DHW) in the post-retrofit building compared to one pump in the original building system.

Even at high cooling and heating loads, the electricity reduction is more than 50% compared to constant speed pumps. This implies that VFDs are beneficial regardless of a building's load profile, though they will show the most improvement in buildings with extended periods of low, non-zero cooling or heating loads.

As is typical of central hydronic systems, the study building also included several constant speed, constant flow pumps, though with smaller and/or more efficient post-retrofit pumps. The nameplate efficiency of the pumps is not the only consideration: Properly sized and selected pumps are more likely to operate near their best efficiency point. The most significant reduction in constant speed, constant flow pump savings was observed in the condenser water pumping: The oversized original pump – providing 2.39 bar dif-

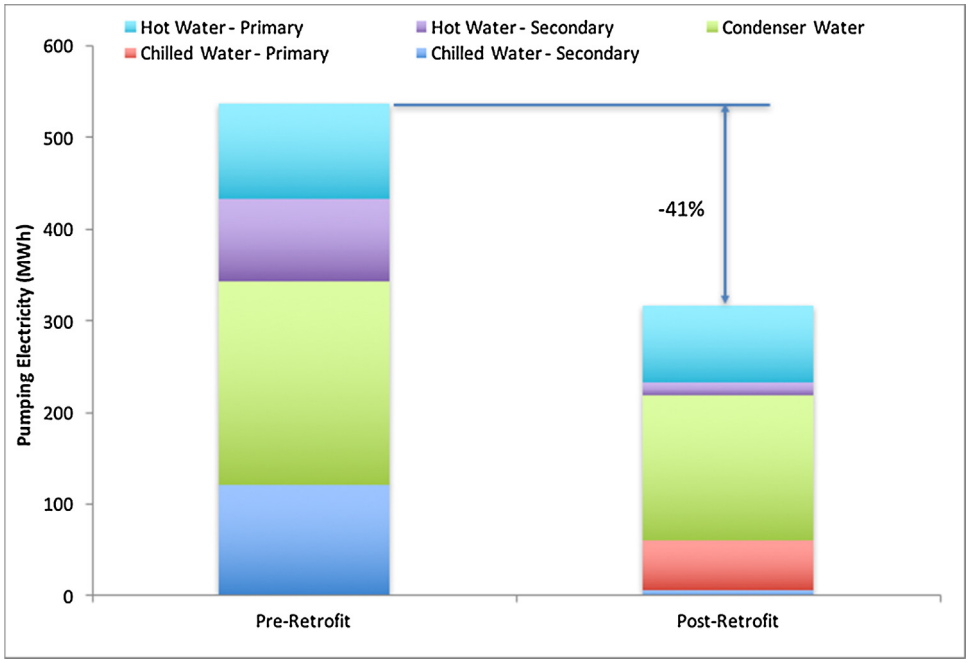

Fig. 14. Total annual central plant system pumping energy and post-retrofit savings.

ferential pressure (80 ft head) at the 0.0704 m^3/s design flow rate with a 22.4 kW (30 hp) motor – was replaced with a smaller pump better suited for the load, providing 1.94 bar differential pressure 1.94 bar (65 ft head) at the design flow rate with a 18.6 kW (25 hp) motor. This resulted in a 27% reduction in constant electric power draw for the largest pumps in the system.

The improperly-sized original chiller-heater HW pumps necessitated that all three of these pumps operate at all times, whereas the upgraded replacement pumps allowed the loads to be met with one pump that provided more head. This resulted in a 20% reduction in constant electric power draw for this service. The original boiler HW pumps were replaced with higher efficiency pumps that provided more head, resulting in a slight increase in constant electric power draw.

The change in the ChW system from a constant primary only (CPO) to a constant primary/variable secondary (CPVS) system necessitated the addition of primary ChW pumps with one running continuously. Total annual ChW pumping energy decreases post-retrofit only if the VFD is in operation due to the additional electricity required to operate the primary pumps.

According to the computed annual electricity usage for all central pumping equipment, the overall retrofit described in this paper resulted in a 41% improvement in pumping energy requirements (23% of all owner-metered electricity usage). Assuming the current building's utility rates for electricity and natural gas, an estimated annual energy savings of approximately 12% of all owner-paid energy bills was computed.

Investigating the individual contributions of system elements and inefficiencies, it was found that the oversizing of the pump has the greatest effect on unnecessarily high power draw requirements, even at the peak cooling load. This is the basis for energy savings associated with VFDs. However, equipment performance and part-load operation alone do not sufficiently capture the inefficiency in the overall building system; additional research is needed to determine the potential for decreases in thermal load to keep occupants comfortable and the most energy efficient means of delivering this service.

Focusing on the electricity usage of hydraulic equipment in hydronic HVAC systems has potential further benefits in reducing energy usage and greenhouse gas (GHG) emissions. By integrating pumps into a control system with communication capabilities, the significant decreases in electricity requirements associated with the VFD controls could provide opportunities for demand management (DM) services and integration with intermittent renewable energy sources, such as wind and solar.

6. Conclusions

This paper describes an investigation of the pumping requirements of a central plant providing cooling, heating and domestic hot water services for a high-rise mixed use, primarily multifamily residential building in New York, NY. The energy impact of various modifications to the waterside components and operation of the hydronic systems were evaluated through a combination of statistical and engineering analytical approaches.

In the U.S., the growth in multi-family buildings is far outpacing single-family construction, and the size of multifamily buildings themselves is increasing. Determining the electricity requirements for pumping in hydronic systems has been identified as a research gap by the U.S. Department of Energy. All central pumping equipment in the original building system used an estimated 537 MWh electricity in the one-year time period studied, 29% of all annual owner-paid utility bills.

The retrofit resulted in a computed annual electricity usage of 316 MWh, a 41% improvement in pumping energy requirements and 12% reduction in all owner-paid energy bills were computed. This indicates very significant energy savings are possible in multifamily building heating and cooling systems even absent thermal envelope improvements or increased efficiency of the heat transfer equipment (e.g. boilers, chillers and terminal units).

VFDs were found to have by far the most significant impact on annual energy usage, providing a 92% reduction in chilled water (ChW) secondary pumping energy. Even with the smaller replacement secondary loop pumps, VFD speeds remained low at higher heating and cooling loads. Because of the oversizing commonplace in the industry, systems essentially always operate at part-load. Given this context, we expect significant energy reduction poten-

tial from installing VFDs on constant flow pumps in addition to those serving variable loads.

This study further illustrates that replacing constant speed pumps with more appropriately sized equipment can significantly reduce their energy usage. Replacing the constant speed, constant flow primary HW and condenser water (CW) pumps provided estimated annual electricity savings of 20% in primary HW pumping and 29% in CW pumping.

Further research using targeted monitoring and the hydronic system characterization approach and analytical methods in this paper would be beneficial to a fast-growing energy demand of interest to industry and policymakers. This should include investigating a cross-section of buildings using different monitoring period lengths and time resolutions with the goal of identifying the accuracy of predictive methods from relatively short monitoring periods. Investigating the effects of similar systems in buildings of different heights would also inform future research.

Acknowledgements

Support for this research was provided by Xylem Inc. The authors would like to specifically like to thank Florin Rosca for his attention to the project, as well as Glenn Huse, Mark Handzel and many others who were involved during the project. The authors would also like to thank Related Companies for their participation in this effort, in particular Luke Falk, Ed Dokovic and other building personnel. This research also could not have been a success without the engineering team at Steven Winter Associates and the numerous contractors involved in bringing the retrofit to fruition.

Appendix.

Table A1
Summary of air handling unit information.

AHU	Area Served	Chilled Water		Hot Water	
		Design Flow (m^3/h)	Valve Control	Design Flow (m^3/h)	Valve Control
1	Residential Corridors	6.4	Modulating	4.6	Modulating
2	Residential Lobby	9.0	Modulating	4.19	Modulating
3	Commercial C	3.5	Two-way	1.7	Two-way
4	Residential Gym	5.11	Two-way	2.8	Two-way
5	Commercial A	19.0	Modulating	6.03	Modulating
6	Commercial A	0.8	None/Open	N/A	None/Open
7	Commercial A	1.8	Two-way	N/A	Two-way
8	Commercial A	1.2	None/Open	N/A	None/Open
9	Commercial B	1.1	Modulating	0.7	Two-way
10	Commercial B	5.5	Two-way	3.5	Two-way
11	Commercial B	2.8	Two-way	1.7	Two-way
12	Commercial B	2.2	Two-way	1.4	Two-way

Table A2
Summary of original and retrofit pumps information.

Pump	Original Pump Ratings/Characteristics				Replacement Pump Ratings/Characteristics			
	Flow (m^3/h)	Pressure (bar)	Motor kW	Pump eff. (%)	Flow (m^3/h)	Pressure (bar)	Motor kW	Pump eff. (%)
P-1	137	2.99	14.9	87.0	137	2.2	11.2	84.4
P-2	137	2.99	14.9	87.0	137	2.2	11.2	84.4
P-3	137	2.99	14.9	87.0	137	2.2	11.2	84.4
P-4	96.6	2.99	14.9	78.8	96.6	2.2	11.2	82.2
P-5	96.6	2.09	11.2	77.5	96.6	2.2	11.2	82.2
P-6	257	2.4	22.4	84.2	258	1.9	18.6	88.0
P-7	257	2.4	22.4	84.2	258	1.9	18.6	88.0
P-8	257	2.4	22.4	84.2	258	1.9	18.6	88.0
P-10	110	1.0	7.5	63.7	110	1.3	7.5	74.6
P-11	110	1.0	7.5	63.7	110	1.3	7.5	74.6
P-12	110	1.0	7.5	63.7	110	1.3	7.5	74.6
P-13	33.8	0.90	1.5	72.4	34.5	1.2	2.2	73.6
P-14	33.8	0.90	1.5	72.4	34.5	1.2	2.2	73.6
P-15	33.8	0.90	1.5	72.4	34.5	1.2	2.2	73.6
P-16	–	–	–	–	137	1.2	7.5	81.0
P-17	–	–	–	–	137	1.2	7.5	81.0

Table A3
Total annual pumping energy estimates for each scenario (all values MWh).

Scenario	Cooling System Pumping					Heating System Pumping		Total System Pumping
	Chilled Water							
	1°	2°	Total	Condenser Water	Total	1°	2°	
Pre-Retrofit	–	121	121	222	324	104	90.5	537
State A	55.2	5.98	61.2	158	218	83.4	13.9	316
State B	55.2	6.42	61.6	158	218	83.4	–	–
State C	55.2	78.1	133	158	279	83.4	–	–
State D	55.2	81.4	137	158	282	83.4	–	–

References

[1] D&R International, Buildings Energy Data Book, 2012, 2011.
[2] E. Bloom, Global Building Stock Database Commercial and Residential Building Floor Space by Country and Building Type: 2011–2021, 2012.
[3] US Census Bureau, Characteristics of New Housing – Multifamily Units, 2015 https://www.census.gov/construction/chars/mfu.html.
[4] B. Donaldson, B. Nagengast, G. Meckler, Heat & Cold: Mastering the Gret Indoors. A Selective History of Heating, Ventilation, Air-conditioning and Refrigeration from the Ancients to the 1930, American Society of Heating, Refrigerating and Air-Conditioning Engineers, Atlanta, GA, 1994.
[5] B. Nagengast, An early history of comfort heating, ACHR News. (2001).
[6] D. Arnold, The evolution of modern office buildings and air conditioning, ASHRAE J. (1999) 40–54.
[7] United Nations, World Urbanization Prospects: The 2014 Revision, Highlights (ST/ESA/SER.A/352), New York, NY, 2014 10.4054/DemRes.2005.12.9.
[8] E.L. Glaeser, Triump of the City: How Our Greatest Invention Makes Us Richer, Smarter, Greener, Healthier, and Happier, Penguin press, New York NY, 2011.
[9] City of New York, Primary Land Use Tax Lot Output (PLUTO), (2011).
[10] D. Westphalen, S. Koszalinski, A.D. Little, Energy Consumption Characteristics of Commercial Building HVAC Systems Volume I: Chillers, Refrigerant Compressors and Heating Systems, 2001.
[11] D. Westphalen, S. Koszalinski, A.D. Little, Energy Consumption Characteristics of Commercial Building HVAC Systems Volume II: Thermal Distribution, Auxiliary Equipment and Ventilation, 1999.
[12] J. Dentz, Building America Expert Meeting Report: Hydronic Heating in Multifamily Buildings, 2011.
[13] W. Goetzler, R. Zogg, J. Burgos, H. Hiraiwa, J. Young, Energy Savings Potential and RD&D Opportunities for Commercial Building HVAC Systems, Navigant Consulting, Inc., Burlington MA, 2011.
[14] W. Goetzler, R. Zogg, J. Young, J. Schmidt, Energy Savings Potential and Demonstration Opportunities for Residential Building Heating, Ventilation, and Air Conditioning Systems, Navigant Consulting, Inc., Burlington MA, 2012.
[15] M. Zaheer-Uddin, P. Monastiriakos, Hydronic heating systems: transiet modeling, validation and load matching control, Int. J. Energy Res. 22 (1998) 33–46.
[16] V. Chandan, G. Zak, A. Alleyne, Modeling of complex hydronic systems for energy efficient operation, in: ASME Dyn. Syst. Control Conf., Hollywood, California, USA, 2013, pp. 1–8.
[17] L. Lianzhong, M. Zaheeruddin, Dynamic modeling and fuzzy augmented PI control of a high-rise building hot water heating system, Energy Sustain Dev. 12 (2008) 49–55, http://dx.doi.org/10.1016/S0973-0826(08)60428-7.
[18] Y.M. Hamam, A. Brameller, Hybrid method for the solution of piping networks, Proc. Inst. Electr. Eng. 118 (1971) 1607, http://dx.doi.org/10.1049/piee.1971.0292.
[19] R. Gamberi, Simulink© simulator for building hydronic heating systems using the Newton–Raphson algorithm, Energy Build. 41 (2009) 848–855, http://dx.doi.org/10.1016/j.enbuild.2009.03.006.
[20] R. Vandenbulcke, L. Mertens, E. Janssen, A simulation methodology for heat and cold distribution in thermo-hydronic networks, Build. Simul. 5 (2012) 203–217, http://dx.doi.org/10.1007/s12273-012-0066-7.
[21] V.B.G. Tavares, E.M. Queiroz, L.H. Costa, R. De Janeiro, F. Uni, E. De Qui, Thermohydraulic simulation of heat exchanger networks, Ind. Eng. Chem. Res. 49 (2010) 4756–4765.
[22] K.N. Rhee, M.S. Yeo, K.W. Kim, Evaluation of the control performance of hydronic radiant heating systems based on the emulation using hardware-in-the-loop simulation, Build. Environ. 46 (2011) 2012–2022, http://dx.doi.org/10.1016/j.buildenv.2011.04.012.
[23] A.A. Bell, HVAC, Equations, Data and Rules of Thumb, 2nd ed., McGraw-Hill, New York, NY, 2008.
[24] American Society of Plumbing Engineers, The Properties of Water and Hydraulics, 2012.
[25] G. Avery, Improving the efficiency of chilled water plants, ASHRAE J. (2001) 14–18.
[26] Lawrence Berkeley national laboratory, Improving Pumping System Performance, U.S Dep. Energy, 2006.
[27] S.T. Taylor, Degrading chilled water plant delta-T, Causes and Mitigation (2002).
[28] T. Walski, K. Zimmerman, M. Dudinyak, P. Dileepkumar, Of variable-Speed pumps with the pump affinity laws, World Water Environ. Resour. Congr. (2003).
[29] R. Carlson, The correct method of calculating energy savings to justify adjustable-frequency drives on pumps, IEEE Trans. Ind. Appl. 36 (2000) 1725–1733, http://dx.doi.org/10.1109/28.887227.
[30] J.B. Maxwell, How to avoid overestimating variable speed drive savings, 27th Ind Energy Technol. Conf. (2005).
[31] B.M.A. Bernier, B. Bourret, Pumping energy and variable frequency drives, ASHRAE J. (1999) 1–4.
[32] Z. Ma, S. Wang, Energy efficient control of variable speed pumps in complex building central air-conditioning systems, Energy Build. 41 (2009) 197–205, http://dx.doi.org/10.1016/j.enbuild.2008.09.002.
[33] E. Costa Bortoni, R.A. Almeida, A.N.C. Viana, Optimization of parallel variable-speed-driven centrifugal pumps operation, Energy Effic. 1 (2008) 167–173, http://dx.doi.org/10.1007/s12053-008-9010-1.
[34] J. Hodgson, T. Walters, Optimizing pumping systems to minimize first or life-cycle costs, in: 19th Int Pump Users Symp, Houston, TX, 2002.
[35] R. Saidur, S. Mekhilef, M.B. Ali, a. Safari, H. a. Mohammed, Applications of variable speed drive (VSD) in electrical motors energy savings, Renew. Sustain. Energy Rev. 16 (2012) 543–550, http://dx.doi.org/10.1016/j.rser.2011.08.020.
[36] P. Fahlén, H. Voll, J. Naumov, Efficiency of pump operation in hydronic heating and cooling systems, J. Civil. Eng. Manage. 12 (2006) 57–62.
[37] W.J. Coad, Variable flow in hydronic systems for improved stability, simplicity, and energy economics, ASHRAE Trans. 91 (1985) 224–237.
[38] A. Yan, J. Zhao, Q. An, Y. Zhao, H. Li, Y.J. Huang, Hydraulic performance of a new district heating systems with distributed variable speed pumps, Appl. Energy 112 (2013) 876–885, http://dx.doi.org/10.1016/j.apenergy.2013.06.031.
[39] Europump, T.H. Institute, U.S.D. of Energy Variable Speed Pumping – A Guide to Successful Applications, 2004.
[40] R. Ruch, P. Ludwig, T. Maurer, Balancing Hydronic Systems in Multifamily Buildings, 2014.
[41] G.P. Henze, W. Henry, M. Thuillard, Improving campus chilled water systems with intelligent control valves: a field study, aei, Asce (2013) 102–111.
[42] T. Durkin, Evolving design of chiller plants, ASHRAE J. 47 (2005) 40–46.
[43] J. Gao, T.F. Smith, Evaluation of hydronic loop energy and modeling of heated water loop containing multiple variable air volume units with hydronic reheat coils, Energy Build. 37 (2005) 189–202, http://dx.doi.org/10.1016/j.enbuild.2004.05.011.
[44] R Core Team, R: A Language and Environment for Statistical Computing, 2016 http://www.r-project.org/.
[45] H. Wickham, Ggplot2: Elegant Graphics for Analysis, Springer-Verlag, New York, 2009.
[46] NFPA, NFPA 101: Life Safety Code, 12th ed., National Fire Protection Association (NFPA), Boston, M ass, 2012.
[47] J.R. Hall, High-rise Building Fires, Quincy, MA, 2013.